AGU PUBLICATIONS

JGR

Journal of Geophysical Research: Space Physics

RESEARCH ARTICLE

10.1002/2014JA020761

Key Points:

- Shock/dynamic pressure excited ULF waves damped in several hundred seconds
- ULF wave energy damping is mainly caused by Landau damping
- The fast damping rate is higher in the plasmasphere boundary layer

Correspondence to:
Q. Zong,
qgzong@pku.edu.cn

Citation:
Wang, C., R. Rankin, and Q. Zong (2015), Fast damping of ultralow frequency waves excited by interplanetary shocks in the magnetosphere, *J. Geophys. Res. Space Physics*, *120*, 2438–2451, doi:10.1002/2014JA020761.

Received 22 OCT 2014
Accepted 9 FEB 2015
Accepted article online 12 FEB 2015
Published online 1 APR 2015

Fast damping of ultralow frequency waves excited by interplanetary shocks in the magnetosphere

Chengrui Wang[1,2], Robert Rankin[2], and Qiugang Zong[1,3]

[1]Institute of Space Physics and Applied Technology, Peking University, Beijing, China, [2]Department of Physics, University of Alberta, Edmonton, Alberta, Canada, [3]Center for Atmospheric Research, University of Massachusetts Lowell, Lowell, Massachusetts, USA

Abstract Analysis of Cluster spacecraft data shows that intense ultralow frequency (ULF) waves in the inner magnetosphere can be excited by the impact of interplanetary shocks and solar wind dynamic pressure variations. The observations reveal that such waves can be damped away rapidly in a few tens of minutes. Here we examine mechanisms of ULF wave damping for two interplanetary shocks observed by Cluster on 7 November 2004 and 30 August 2001. The mechanisms considered are ionospheric joule heating, Landau damping, and waveguide energy propagation. It is shown that Landau damping provides the dominant ULF wave damping for the shock events of interest. It is further demonstrated that damping is caused by drift-bounce resonance with ions in the energy range of a few keV. Landau damping is shown to be more effective in the plasmasphere boundary layer due to the higher proportion of Landau resonant ions that exist in that region.

1. Introduction

Wave-particle interactions involving ULF standing waves [*Dungey*, 1955] can dramatically alter the behavior of electrons [*Zong et al.*, 2007, 2009] and ions [*Yang et al.*, 2010, 2011b; *Zong et al.*, 2011] in the inner magnetosphere. These waves can be excited by external solar wind disturbances and/or internal plasma instabilities. External sources include solar wind dynamic pressure pulses [*Kepko and Spence*, 2003; *Hudson et al.*, 2004; *Takahashi and Ukhorskiy*, 2007; *Claudepierre et al.*, 2009, 2010, 2013], Kelvin-Helmholtz (K-H) instabilities on the magnetopause [*Hudson et al.*, 2004; *Claudepierre et al.*, 2008], and ion cyclotron resonance with back-streaming solar wind ions [*Odera*, 1986]. The K-H instability can excite ULF waves in the magnetosphere through coupling that takes place between long-wavelength surface-mode waves and earthward field line resonances (FLRs) [*Fairfield et al.*, 2000; *Hasegawa et al.*, 2004; *Rae et al.*, 2005; *Claudepierre et al.*, 2008]. Interplanetary shocks and solar wind dynamic pressure pulses also excite ULF waves, although the precise mechanism that converts shock energy to waves of high azimuthal wave number (high-*m*) is not yet fully understood. A possible mechanism related to substorm injections has been discussed by *James et al.* [2013]. In this paper we put aside the issue of how these waves are generated and focus on the wave-particle interactions they cause.

ULF waves excited by shocks and dynamic pressure variations can be very intense and are sometimes damped away quickly over tens of minutes [*Zong et al.*, 2009; *Zhang et al.*, 2010]. In this paper, it is shown that the observed fast damping is caused by drift-bounce resonance between ULF waves and ions having energies of a few keV. Such a mechanism has been described theoretically by *Southwood and Kivelson* [1981, 1982] and is possible because of the comparable periods of drift and bounce motion of energetic particles and ULF oscillations. As reported by *Yang et al.* [2010, 2011a, 2011b] and *Zong et al.* [2011], the associated damping takes place over time intervals where wave electric fields accelerate charged particles, a process that can also enhance radial diffusion [e.g., *Loto'aniu et al.*, 2006]. Although energetic particle drift-bounce resonance may occur with different ULF modes, e.g., toroidal ULF waves [*Elkington et al.*, 1999] and compressional poloidal-mode ULF waves [*Elkington et al.*, 2002, 2003, 2004; *Tan et al.*, 2011], the interaction with poloidal ULF waves [*Zong et al.*, 2009, 2011, 2012] is considered to be more efficient [*Zong et al.*, 2009; *Yang et al.*, 2011a, 2011b; *Zong et al.*, 2012], even leading to the formation of a new radiation belt [*Li et al.*, 1993; *Wygant et al.*, 1994; *Zong et al.*, 2011] in certain situations. It has been reported by *Zong et al.* [2007, 2009] and *Tan et al.* [2004, 2011] that acceleration of electrons by drift-bounce resonance can also take place.

In the auroral zone, *Wright et al.* [2003] studied FAST satellite data and showed that electron acceleration can dissipate an amount of energy similar to joule heating. Dispersive-scale Alfvén wave damping has been investigated by *Lysak and Lotko* [1996], who showed through analysis of the kinetic wave dispersion relation that Landau damping by electrons can be efficient at spatial scales where electron inertia and finite ion gyroradius become important. In a different context, *Evans et al.* [2009] evaluated the importance of Landau damping for surface Alfvén waves in the solar wind. Important as these studies are, they have not quantified Landau damping in regions of the magnetosphere where standing Alfvén waves and FLRs are common. One such attempt was made by *Rankin et al.* [2007], who showed through numerical simulations that electron particle trapping can be efficient in suppressing Landau damping in short perpendicular-scale standing ULF waves. Another approach was considered by *Hollweg* [1971], who calculated the nonlinear Landau damping rate of Alfvén waves based on theoretical considerations of *Stix* [1992]. A general approach to estimate the damping rate of standing ULF waves has been given by *Southwood* [1976], who examined the drift-bounce mechanism, which is the subject of the study presented here.

Besides Landau damping, other ways of energy loss from ULF waves include joule heating in the ionosphere and the propagation of wave energy through the magnetospheric waveguide. Joule heating of ionospheric particles through Alfvén waves has been widely studied and is usually considered the most effective energy sink. For example, *Newton et al.* [1978] numerically computed the damping rate for ULF waves for different height-integrated Pedersen conductivity, whereas *Greenwald and Walker* [1980] studied in detail the amount of energy loss in a particular ULF event. More sophisticated models [*Sydorenko and Rankin*, 2012] describing the propagation of ULF waves in the ionosphere have also been developed. Two-dimensional MHD computer models by *Sciffer et al.* [2005] and *Waters and Sciffer* [2008] include solutions for near-vertical magnetic fields at high latitudes and for oblique magnetic fields applicable at lower latitudes. Observationally, *Rae et al.* [2007] found that more than 30% of the energy in FLRs was deposited via joule heating during a substorm cycle. The same authors estimated that joule heating can be an effective means of transporting energy from the solar wind into the high-latitude ionosphere. Another mechanism of energy loss from ULF waves was considered by *Wright* [1994], who studied transport of waves through the magnetospheric waveguide. A related study by *Claudepierre et al.* [2008] studied transport of low-m ULF waves generated by the Kelvin-Helmholtz instability in a numerical simulation.

In this paper, we study the temporal variation of shock-excited ULF waves under different damping mechanisms. Comparing the effects of Landau damping, joule heating, and waveguide propagation, we find that the evolution of wave energy cannot be fully accounted for by joule heating or waveguide propagation. We further show that in certain situations the Landau damping rate of Alfvén waves is higher than from joule heating, i.e., as a result of fundamental-mode ($N=2$) drift-bounce resonance with energetic ions. Our results suggest that Landau damping can induce fast damping of ULF waves when the drift-bounce resonance mechanism is effective, i.e., when particles in sufficient numbers satisfy the resonance condition. To our knowledge, we present the first reported explanation for the strong damping of ULF waves that can accompany interplanetary shocks.

The paper is organized as follows: The second section describes two representative observations of fast damping of Alfvén waves in different regions of the magnetosphere. In the third section, we compare wave propagation, Landau damping, and joule heating. Finally, we suggest that the Landau damping mechanism is more effective for some regions of the magnetosphere because such regions can support generation and/or propagation and damping of ULF waves excited by shocks without modifying the frequency of Alfvén waves. This feature is a characteristic of the observations we consider.

2. Observations

The magnetic and electric field data for ULF waves presented in this paper are obtained from the Fluxgate Magnetometer and Electric Field and Wave (EFW) experiment on the Cluster II satellite constellation [*Balogh et al.*, 2001]. The plasma density is calculated from the EFW experiment using the method from *Moullard et al.* [2002]. The four Cluster spacecraft are capable of observing three-dimensional, small-scale spatial structure in the space environment, including electromagnetic fields and particles. We present two shock-induced Alfvén wave events for detailed study.

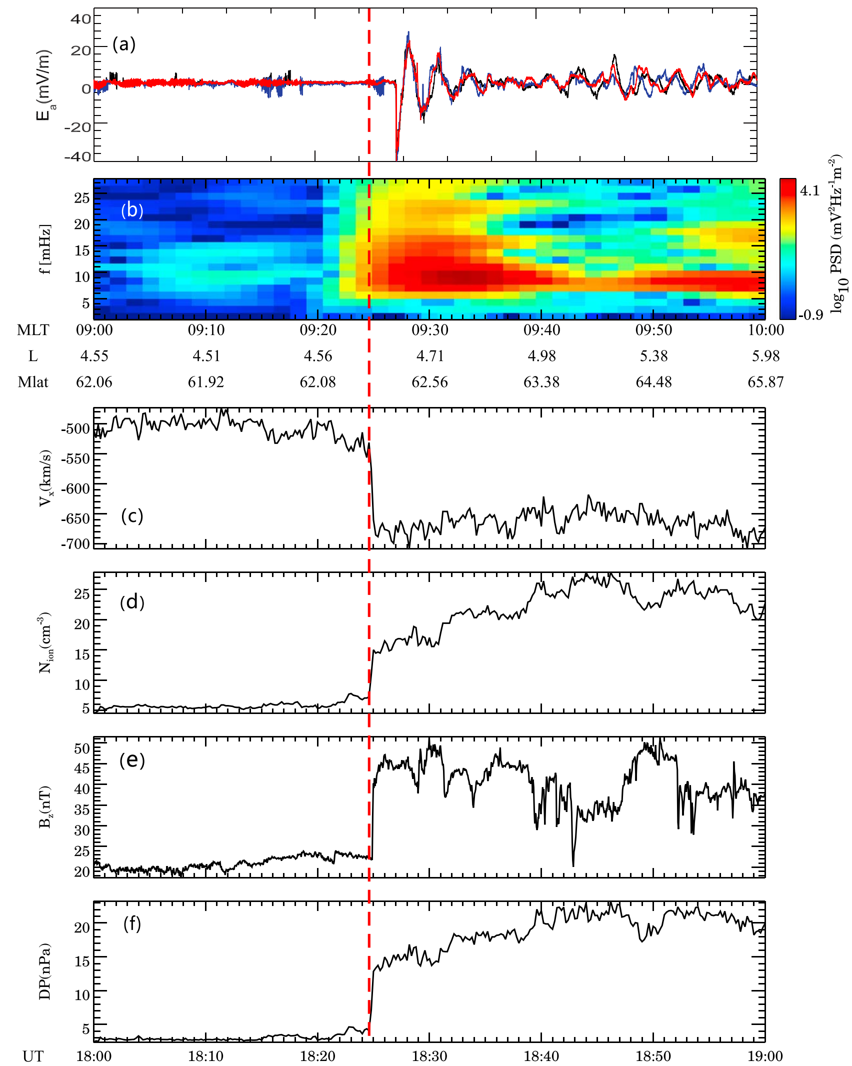

Figure 1. The overview of a shock event and the following ULF waves observed on 7 November 2004 from 18:00 UT to 19:00 UT. (a) Azimuthal component of electric field observed by Cluster spacecraft; black, red, and blue lines are the observations of C1, C2, and C4 respectively. (b) The electric field dynamic power spectrum from C1. (c) *x* component of solar wind velocity. (d) Solar wind ion density. (e) *z* component of interplanetary magnetic field. (f) Dynamic pressure of solar wind. Figures 1c–1f are observations from Geotail satellite. Geotail observed a shock event, and Cluster observed the energy enhancement of ULF waves around the same time. Red dashed line indicates the arrival of interplanetary shock.

2.1. Fast Damping of a Large-Amplitude ULF Wave in the Plasmasphere Boundary Layer

First of all, we focus on the shock event on 7 November 2004. Figure 1 gives an overview of this event. An interplanetary shock hit the magnetosphere through a sudden increase in maximum solar wind dynamic pressure and plasma density at 18:27 UT. The locations of spacecraft are shown in Figures 2a and 2b. During the event, Geotail was upstream in the solar wind at (19.28, 13.59, −2.66) R_e in GSE coordinates. The magnitude of the solar wind velocity *x* component V_x increased from about 550 km/s to 700 km/s. The ion density increased from about 8 cm^{-3} to 15 cm^{-3}. The *z* component of the interplanetary magnetic field B_z increased by about 15 nT. The dynamic pressure of the solar wind continually increased after the arrival of the shock and reached more than 70 nPa. An intense magnetic storm with minimum *Dst* of −373 nT followed the shock [*Tsurutani et al.*, 2008].

ULF waves accompanying shocks, especially Pc5-ULF waves, are usually excited in the dayside of the magnetosphere [*Hudson et al.*, 2004; *Brito et al.*, 2012] but propagate to the nightside at the fast-mode speed [*Wygant et al.*, 1994]. On 7 November 2004, the Cluster satellites observed ULF waves generated

10.1002/2014JA020761

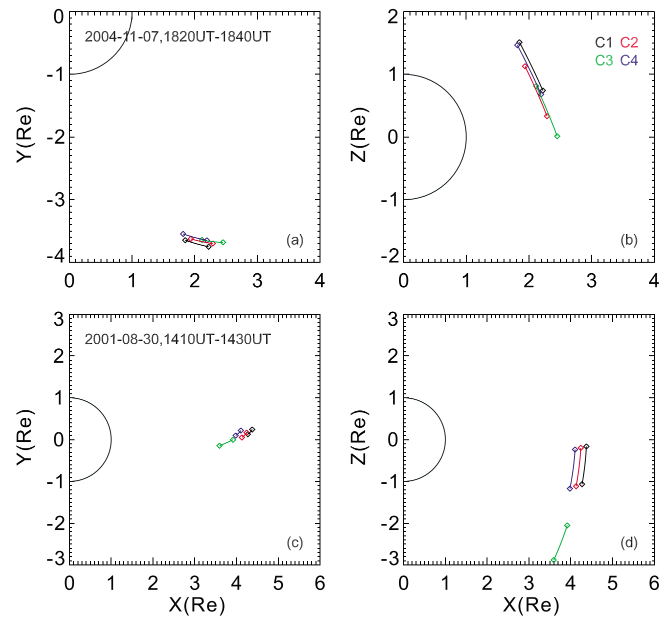

Figure 2. (a) Orbits of Cluster spacecraft in *X-Y* plane on 7 November 2004 from 18:20 UT to 18:40 UT. (b) Orbits of spacecraft in *X-Z* plane in the same time range as Figure 2a. (c) Orbits of Cluster spacecraft in *X-Y* plane on 30 August 2001 from 14:10 UT to 14:30 UT. (d) Orbits of spacecraft in *X-Z* plane in the same time range as Figure 2c. Orbits of C1, C2, C3, and C4 are shown in black, red, green, and blue lines, respectively. All orbits are shown in GSE coordinates.

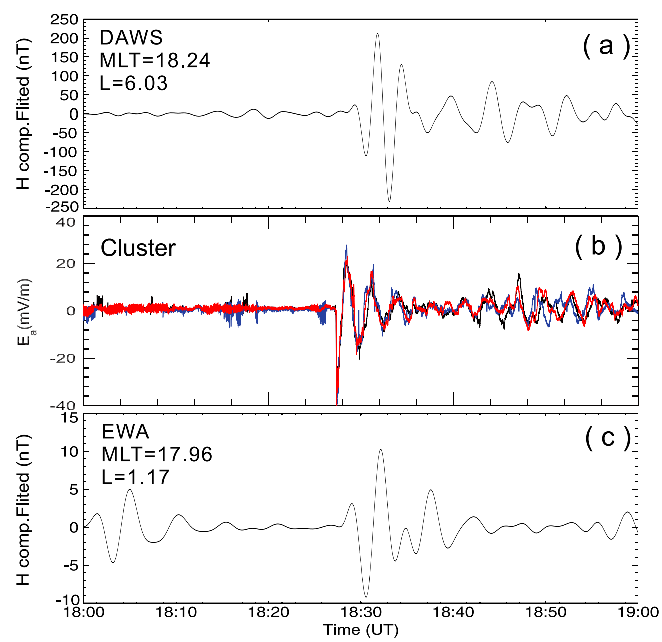

Figure 3. (a and c) Band-filtered north-south component of geomagnetic field fluctuation. The elliptic band-pass filter is used, and the filter band is between 3 mHz and 8 mHz. Data to make Figure 3a are from Dawson City (DAWS) station of CARISMA magnetometer network. Data to make Figure 3c are from Ewa Beach (EWA) of station 210 magnetic meridian magnetometer network. (b) Azimuthal component of electric field observed by Cluster spacecraft in similar format as Figure 1a. The three panels are arranged along the geomagnetic latitude of the footprint of satellite or the station.

after a shock, while the Cluster fleet was traveling in the morning side of the plasmasphere boundary layer (around 09:00 magnetic local time (MLT), $L = 4.5$). Figure 1 shows the observation of the azimuthal component of the electric field (E_a) in a local mean field-aligned coordinate system [*Takahashi et al.*, 1990] and the corresponding x component of solar wind velocity (V_x) during the period from 18:00 to 19:00 UT. The observed quasi-sinusoidal electric field with a period of about 3 min had a peak amplitude of 10 mV/m and was attenuated over time. Figure 3 shows a comparison between satellite and ground observations in this event. Along adjacent flux tubes, both the ground and the satellite observed amplitude attenuate over a similar time range. The power spectral density (PSD) of E_a is shown in Figure 1b and was obtained using dynamic spectral analysis [*Takahashi and Ukhorskiy*, 2007]. The central frequency of ULF waves is observed to be about 6.7 mHz. The PSD is also strong at a frequency around 17 mHz, which may be due to a higher harmonic resonance of 6.7 mHz. In this particular event, the azimuthal wave number for the poloidal mode was estimated to be around 50, with the wave propagating eastward [*Zong et al.*, 2009]. In the process of wave generation and damping, particles have been accelerated by ULF waves in this event as described by *Zong et al.* [2009]. It will be demonstrated that the interaction between particles and waves, especially resonant processes, can be a main factor in explaining the damping of the observed Alfvén waves in this event.

2.2. Fast Damping of Moderate-Amplitude ULF Waves in the Plasmasphere and Plasmasphere Boundary Layer

Figure 4a shows shock-excited electric field variations measured by Cluster on 30 August 2001. During the event, the spacecraft were in the outer radiation belt with $L \sim 4.5$

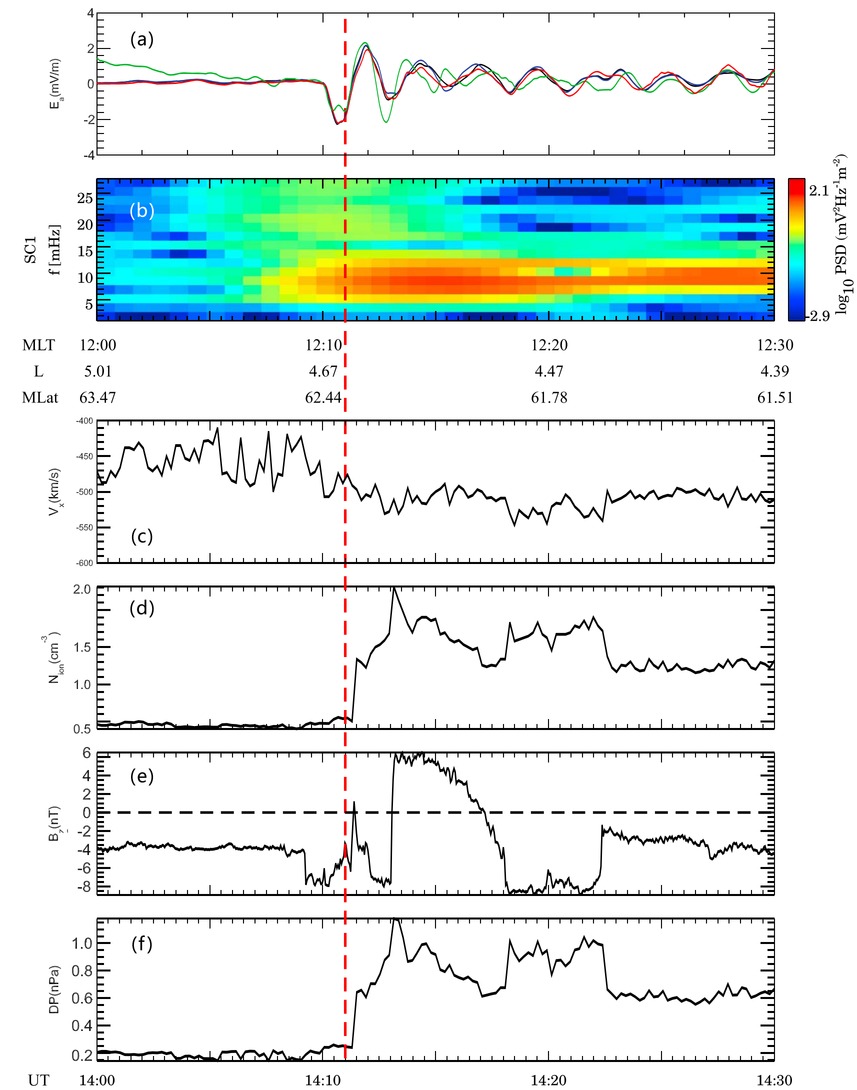

Figure 4. The overview of a shock event and the following ULF waves observed on 30 August 2001 from 14:00 UT to 14:30 UT. (a–d) Similar format as Figure 1. Black, red, green, and blue lines are the observations of C1, C2, C3, and C4, respectively, in Figure 4a. Shock arrived at about 14:10 UT, and Cluster observed small-amplitude ULF waves.

(C1, C2, and C4) at about 12:00 MLT. The locations of spacecraft are shown in Figures 2c and 2d. C3 crossed into the plasmasphere boundary layer, while the other three spacecraft were in the plasmasphere proper. The Geotail spacecraft were located at (15.19, −12.15, −1.13) R_e in GSE coordinates when they observed the shock: the plasma density increased to 1.5 cm^{-3}, the amplitude of solar wind velocity increased from 450 km/s to 550 km/s, and the dynamic pressure increased from about 0.2 nPa to about 1.0 nPa. This event was induced by a weaker interplanetary shock than the one in 2004. The oscillations of the electric field azimuthal component were about 1.5 mV/m in this case and were attenuated over a few minutes. The central frequency with the largest power density was in the ULF range (about 7.8 mHz). In this event, the azimuthal wave number for the poloidal mode is estimated as 10 ± 3 [*Eriksson et al.*, 2006], with the wave propagating eastward.

The observed magnetospheric plasma density variation is shown in Figure 5a. The density of ions in the plasmasphere bounday layer was about 8 cm^{-3} at C3 while being over 100 cm^{-3} in the location of C1, C2, and C4, which were in the plasmasphere. Such large differences in densities between the plasmasphere boundary layer and plasmasphere can induce distinct waves in the plasmasphere. Figure 5 shows wavelet analysis results for different satellites, where the electric field components have been converted into the mean field-aligned coordinate system. E_a corresponds to the poloidal mode of ULF waves, assuming

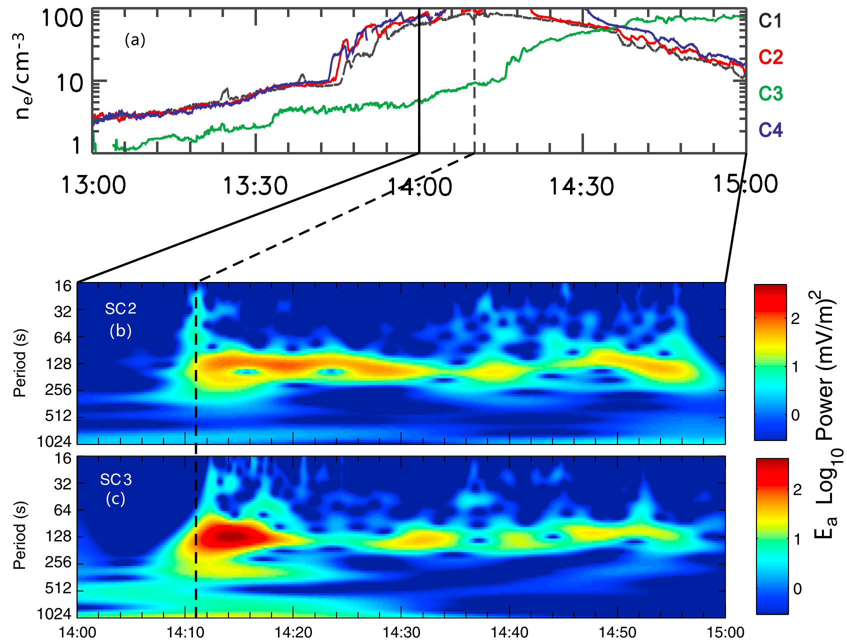

Figure 5. Observations of ULF waves inside the plasmasphere and in the plasmasphere boundary layer for the event on 30 August 2001. (a) The plasma density calculated from spacecraft potential measured by EFW instrument on Cluster. C1, C2, C3, and C4 are shown in black, red, green, and blue lines, respectively. C3 was in the plasmasphere boundary layer, and the other three spacecraft were in the plasmasphere. By comparing the wavelet spectrum analysis results from (b) C2 and (c) C3, we see that wave energy is damped faster in C3.

a dipolar geomagnetic field. Spacecraft C2 and C3 observed a power density increase for waves in the 5–10 mHz range. The power of the waves observed by C3 is larger than that observed by C2, while their rate of decay (damping) is much faster than at C2. At 14:12 UT, C3 observed an electric field with fluctuations exceeding 100 $(\mathrm{mV/m})^2$ with a period of about 128 s, decreasing to about 10 $(\mathrm{mV/m})^2$ at around 14:20 UT. As for spacecraft C1, the power density of the electric field fluctuations decreased to 10 $(\mathrm{mV/m})^2$ after 14:30 UT. This difference may be reflected by the spatial separation of the two spacecraft, which sample a different local density and energy of particles. Previous studies have pointed out that the density gradient in the plasmasphere boundary layer should have an effect on VLF waves [*Wang et al.*, 2011], and this appears to be true also for ULF waves. The expected change in amplitude of ULF waves across the plasmapause was also discussed by *Allan and Knox* [1979] and *Menk et al.* [2004].

According to *Fraser et al.* [2005], the plasma mass density distribution near the plasmasphere boundary layer can affect the characteristics of ULF waves. But how it affects ULF wave damping has not yet been fully analyzed. The Alfvén velocity $V_A = B(s)/\sqrt{\mu_0 \rho(s)}$ (where μ_0 is the vacuum permeability and B is the magnetic field) depends on the plasma mass density $\rho(s)$ along field lines, and consequently, the frequency and propagation characteristics of ULF waves is affected as the waves propagate through the plasmasphere boundary layer. It is also known that oxygen ions contribute significantly to mass loading along the field line during disturbed periods, which is another consideration at later times as the ring current develops [e.g., *Jordanova et al.*, 1996].

3. Interpretation and Discussion: Possible Mechanisms for Fast Damping of ULF Waves

3.1. Joule Heating

Ionospheric damping of Alfvén waves is one of their main sinks of energy. The damping takes place through joule heating produced by the interaction of the waves with ionospheric particles. For a transverse wave, joule dissipation through Pedersen currents can be calculated based on a boundary condition at the ionosphere: $b = \mu_0 \Sigma_P E$, where Σ_P is the height-integrated Pedersen conductivity. This boundary condition

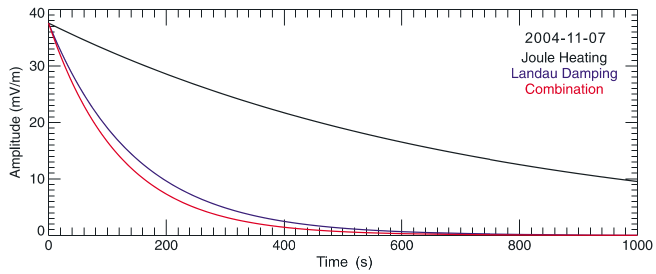

Figure 6. The variations of ULF waves amplitude caused by different damping mechanism. Black, blue, and red lines are the calculated damping rates at C3, based on joule heating, Landau damping, and the combined effect, respectively.

can also be written in another form [*Southwood and Hughes*, 1983]:

$$\frac{Eb}{\mu_0} = \Sigma_P |E|^2. \tag{1}$$

In this equation, joule heating is balanced by net Poynting flux into the ionosphere. In the events of interest, damping rates are calculated according to the simple model of *Newton et al.* [1978]. Although more sophisticated and more recent numerical models of ULF wave propagation in the ionosphere have been developed, we use Newton's calculations because it provides simple analytical expressions for damping that are valid for high-m waves and near-vertical geomagnetic field, assumptions that hold for the events we are studying. As we shall see later, the damping rates for joule heating turn out to be much smaller than Landau damping, and so it is reasonable to expect that our conclusions will not change on using more complex models of damping. *Newton et al.* [1978] calculated the damping rate of Alfvén waves due to joule heating and found that when the Pedersen conductivity is large ($\Sigma_P > 1$S) in the dayside ionosphere, low harmonic poloidal Alfvén wave damping occurs at the rate $\gamma/\omega = 2.2 \times 10^{-2} \Sigma_P^{-1} L^{3/2}$.

Using this last result, the damping rate of ULF waves in both shock events studied can be estimated based on a height-integrated conductivity calculated from the IRI2012 model (http://wdc.kugi.kyoto-u.ac.jp/ionocond/sigcal/index.html). The estimated damping rate at C1 is $\gamma/\omega \simeq 0.028$. The effect of ULF wave damping produced by joule heating is shown in Figure 6. The wave amplitude reduces to 30% of the initial amplitude over the time indicated, and the calculated damping rate is similar in both C1 and C3 in the 2001 event. Although joule heating is an effective damping mechanism, the two observations reported here reveal that the observed damping is much faster than can be provided by joule heating alone.

3.2. ULF Wave Damping Through Drift-Bounce Resonance

As discussed earlier in the paper, Landau damping of large-amplitude standing Alfvén waves in geomagnetic fields can occur through wave-particle interactions. It represents an additional damping on waves over joule heating. The most important interaction between charged particles and ULF waves, especially poloidal ULF waves, is drift-bounce resonance. The resonance condition can be written as [*Southwood et al.*, 1969]:

$$\omega - m\omega_d = N\omega_b, \tag{2}$$

where ω, ω_d, and ω_b are wave frequency, particle drift frequency, and bounce frequency, respectively; m is the azimuthal wave number; and N is an integer that depends on the harmonic mode of the standing wave. In each full bounce in latitude the particle moves westward exactly N wavelengths in the frame of the wave. In the two events studied, electric field of shear Alfvén waves are observed near the equator or at medium-latitude region. We choose a fundamental mode with $N=2$ as representative of the events. According to *Southwood and Kivelson* [1982], *Chen and Hasegawa* [1988], and *Southwood et al.* [1969], the electric field seen by an ion in drift-bounce resonance (in this case with an $N=2$ high-m ULF wave) will cause damping or growth of the wave as it maintains the same direction as the ion bounces between hemispheres. The resonance energy for different ions can be calculated from equation (2) because ω_d and ω_b are dependent on the particle energy E [*Baumjohann and Treumann*, 1997] and take the following form in a dipole magnetic field:

$$\omega_b = \frac{(W/m)^{1/2}}{LR_E}(0.59 - 0.25 \sin \alpha_{\mathrm{eq}})^{-1}, \tag{3}$$

$$\omega_d = \frac{LW}{qB_E R_E^2}(2.1 + 0.9 \sin \alpha_{\mathrm{eq}}), \tag{4}$$

where α_{eq} is the pitch angle of a particle at the equatorial region. By substituting equations (3) and (4) into equation (2), the resonance condition can be obtained once the azimuthal mode number m is specified.

10.1002/2014JA020761

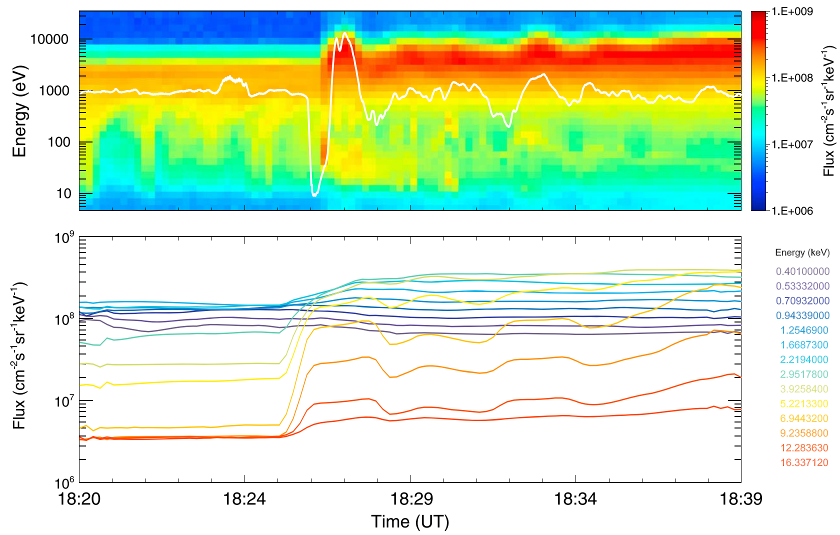

Figure 7. The resonance between ULF waves and ions in the 2004 event. (top) Ion spectrum overlaid with electric field oscillations for the 2004 shock event. (bottom) The flux in several energy channels as a function of time.

The azimuthal wave number can be calculated from multispacecraft data using the technique of *Takahashi et al.* [1985]:

$$m = \frac{\Delta\theta}{\Delta\phi}, \tag{5}$$

where $\Delta\theta$ and $\Delta\phi$ are, respectively, the cross-phase difference in the time series, and the azimuthal separation of satellites. In the 2004 event, the m-value is estimated to be 50 for the poloidal mode [*Zong et al.*, 2009, 2012]. Combining the m-value of poloidal ULF waves with the spatial separation of the spacecraft, the resonance energy expected for oxygen ions in interaction with a 7.8 mHz is between 8.85 keV and 12.74 keV in the pitch angle range of 45–75°. For H ions the resonance energy is between 2.67 keV and 4.45 keV.

The bounce frequencies of energetic electrons with energy of tens of keV in the inner magnetosphere are much higher than either the energetic electron drift frequency or the Pc5 wave frequency [*Zong et al.*, 2009]. Thus, the drift-bounce resonance of energetic electrons can only be excited with $N=0$. The condition for resonance changes into

$$\omega = m\omega_d. \tag{6}$$

For electrons interacting with poloidal-mode waves, the resonant energy requirement is lowered because of their typically large m-value ($m \sim 50$). The resonance energy of electrons corresponds to $E_{Re^-} = 110.1$ keV. From the considerations and estimates presented above, hydrogen ions resonate at the lowest energy, followed by oxygen, and then electrons. The approximate damping rate can be calculated following *Southwood* [1976]:

$$\frac{\gamma}{\omega} = \frac{\rho_{\mathrm{res}} V_{\mathrm{res}}^2}{\rho\omega^2 L^2}, \tag{7}$$

where γ is the damping rate, ω is the frequency of the wave, ρ and v are particle density and velocity, and the suffix "res" refers to the particle in resonance. This ULF wave damping rate requires assumptions of finite plasma β and an axisymmetric field with mirror symmetry. Around $L \sim 4$ the magnetic field can be considered a dipole field, and so the model assumptions are valid for the observations of interest in this study. Although the damping rate derived by *Southwood* [1976] is approximate, it provides by far the largest damping rate and can explain the observed difference in damping between waves excited in the plasmasphere and plasmasphere boundary layer.

The particle differential flux can be computed using data from the CIS (Cluster Ion Spectrometry) and RAPID (Research with Adaptive Particle Imaging Detectors) instruments on Cluster, as illustrated in Figure 7.

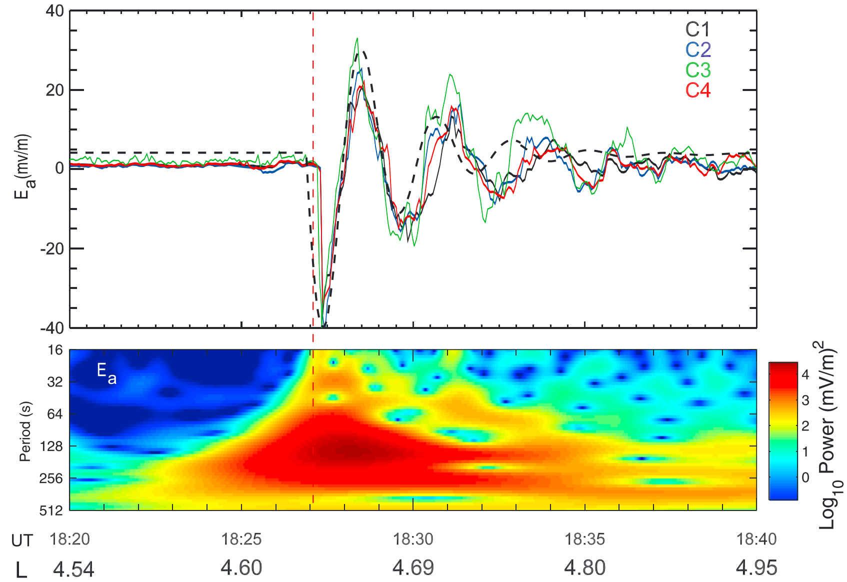

Figure 8. (top) The azimuthal component of electric field observed by Cluster in the 2004 event. Black, blue, and red lines are the observation C1, C2, and C4, respectively. The black dashed line multiplies the maximum amplitude by the damping rate calculated from equation (2). (bottom) Wavelet analysis spectrum of C3 observed electric field azimuthal component.

Figure 7 (top) shows ion energy flux overlaid with electric field oscillations for the 2004 shock event. Figure 7 (bottom) shows the flux in several energy channels as a function of time. There is a resonance peak between 6.94 keV and 9.23 keV that brackets the resonant energy expected for O+, i.e., between 8.85 keV and 12.74 keV in the pitch angle range of 45–75°. The corresponding resonant energy for H+ is between 2.67 keV and 4.45 keV, while for electrons it is between 77.03 keV and 109.1 keV. The ion flux data, especially the contribution from O+, provides evidence of a link between the observed strong damping of waves and drift-bounce resonant wave-particle interactions. In the event pertaining to this figure, the relative density ρ_{res}/ρ is about 0.0143, where ρ_{res} can be computed using data from the CIS and RAPID instruments on Cluster. The calculated damping rate corresponds to $\gamma/\omega \simeq 0.117$, which is much larger than the damping rate induced by joule heating. The effects of Landau damping and joule heating are compared in Figure 6. It can be seen that the amplitude of ULF waves is damped to below 3.2% of the original amplitude in 600 s if there is only Landau damping. The combined effect of both mechanisms can damp the ULF wave to 1.4% of the initial amplitude in the same time span. The conclusion is that fast attenuation of the observed wave amplitude is mainly caused by Landau damping.

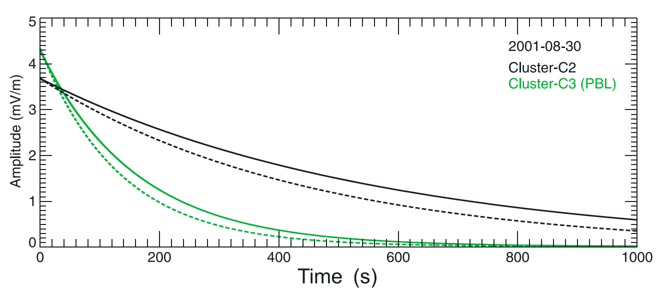

Figure 9. The variations of ULF waves amplitude inside and outside of plasmasphere. Black and green lines are the calculated damping rates at C2 and C3, respectively, for the 2001 event. They show that the Landau damping rate of ULF waves is largely affected by satellite position in the magnetosphere. The dashed lines indicate the damping rate in considering both of joule heating and Landau damping.

The results calculated from Cluster in the case of the 2004 event with the combined effect of Landau damping and joule heating are shown in Figure 8. We choose the maximum amplitude of the electric field as the initial wave amplitude and assume that damping proceeds from the time the maximum field is attained. The results are based on equation (7) and the observed frequency of ULF waves. Compared with the observation, the calculated damping rate gives a good fit to the observation. This demonstrates that the main part of the energy loss of Alfvén waves is due to bounce-resonant Landau damping in this event.

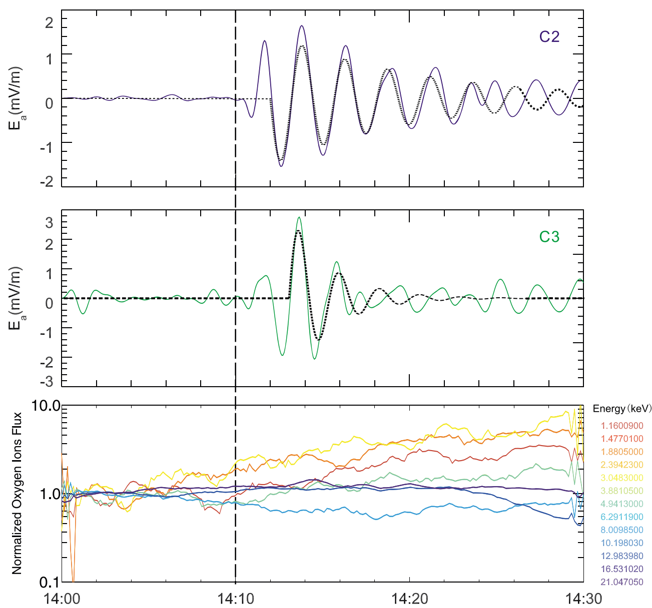

Figure 10. (top) The azimuthal component of electric field observed by Cluster C2 in the 2001 event. The blue line is the observation of C2. (middle) The same format as C3, while the green line is the observation of C3. (bottom) The flux of oxygen ions in different energy channels as a function of time. The flux in each energy channel has been divided with the average flux before the shock arrival (the average flux between 1400 UT and 1408 UT) in order to show the variation of each channel.

In the 2001 event, variations of electron number density imply that C3 was in the plasmasphere boundary layer region and C2 was in the plasmasphere. This allows us to consider damping rates of ULF waves in different regions of the magnetosphere. The estimated and observed damping rates are shown in Figures 9 and 10. In this event, the resonant energy expected for O+ is between 1.71 keV and 5.36 keV. This is consistent with a resonant response in ion flux oscillations in the satellite energy channel between 1.16 keV and 3.04 keV. In Figure 9, the dashed lines and the solid lines show the damping rate with and without joule heating, respectively. It can be seen that in the 2001 event, Landau damping is also the main damping mechanism in both the plasmasphere and the plasmasphere boundary layer. As the damping rate caused by joule heating depends on the ionospheric conductivity at the end of field lines, there is no significant difference in joule heating rates between C2 and C3. According to the observations shown in Figure 5, however, the ULF oscillations of C3 damped faster than those at the other satellites. Although C3 observed a larger-amplitude maximum, it damped much faster within 600 s, by which time the amplitude of C3 was below 0.1 mV/m, while that of C2 was still around 1.4 mV/m. A more detailed comparison between the observations and estimation of damping is shown in Figure 10. The 4–9 mHz band-filtered ULF waves and the calculated damping curve are very close to each other in both the C2 and C3 observations. The different damping rates between C2 and C3 is likely caused by the different plasma densities at the position of C2 and C3 in the magnetosphere. The implication is that due to a dependence of the damping rate on density, wave energy is transferred into particle energy at a lower rate at C2. This can be inferred from equation (7), which shows that the proportion of particles in resonance is the main factor in determining the damping rate. This proportion was smaller in the plasmasphere because the overall particle density was higher in the plasmasphere. Regardless, Landau damping is the main factor in explaining the different damping rate in the plasmasphere and plasmasphere boundary layer.

3.3. Energy Propagation in the Magnetospheric Waveguide

In this section we consider the possibility that shear Alfvén waves observed by Cluster are field line resonances (FLRs) excited through mode conversion of compressional waves that propagate in the magnetotail waveguide. The compressional waves will lose amplitude as they propagate, and this will manifest as an apparent damping of shear waves observed by the satellites. As FLRs can be reasonably approximated as 1D eigenmodes of standing wave electric and magnetic fields, this is consistent with the approach used to estimate Landau and ionospheric damping. We will estimate and compare damping as a result of wave propagation with joule heating and Landau damping. The estimates provided are based on a point-like source of waves, which should correspond to the strongest level of damping.

Figure 11 is a schematic diagram of the magnetospheric waveguide viewed in the ecliptic plane according to *Wright* [1994]. A point-like source of fast-mode waves in the waveguide will propagate energy isotropically throughout the magnetosphere. The wave energy arriving earliest in time at the observation point (satellite) will have traveled along a path of minimum distance between the source and the observation point; it will therefore have the largest amplitude, having spread out the least. Wave energy arriving at the observation point after reflection from the boundaries of the waveguide will arrive at the satellite with

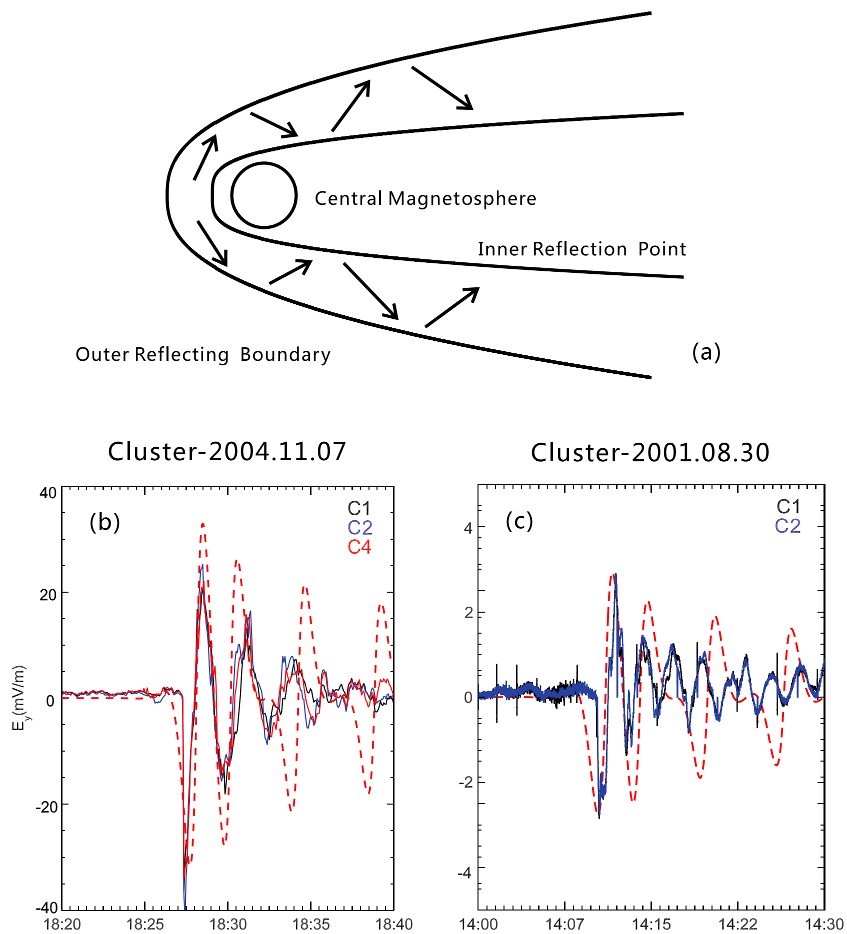

Figure 11. (a) The progress of the compressional waves propagation in the waveguide of magnetosphere [from *Wright*, 1994]. (b) Comparison between the calculated waveguide-caused damping and the observation from Cluster for the event in 2004. (c) Similar comparison between calculation and observation from Cluster for the event in 2001.

correspondingly smaller amplitude. Even if energy dissipation is neglected, the observed wave amplitude would appear attenuated because the amplitude versus time at the observation point represents arrival of waves along paths corresponding to fast-mode waves that are increasingly spread out. *Wright* [1994] calculates this effect and gives an expression for the damping of wave amplitude,

$$b_z \propto b_{z0}/R^{1/2}, \tag{8}$$

where R is the propagation distance from the wave source to the satellite accounting for wave reflection and b_{z0} is the amplitude of the fast-mode wave at the source point. Here we assume that the medium is uniform. For different wave packets with different initial wave normal direction **k**, their arriving times are discrete at a specified observation point. A wave leaving the center of the source region and bouncing off the boundaries j times will traverse a distance in x of jx_m. Only when j is an integer will the wave packet arrive at the observation point. According to equation (8) from *Wright* [1994],

$$t = \sqrt{y_0^2 + j^2 x_m^2}/V, \tag{9}$$

where y_0 is the distance between the source and the observation point along the waveguide and x_m is the width of waveguide. This feature is not consistent with our observation. In Figure 11, we consider damping of a single-frequency source. Here the estimate of damping neglects mode conversion caused by reflection from the inner magnetosphere turning point. As a result of this process, wave energy can be absorbed depending on the angle of incidence of the fast-mode wave as it approaches the turning point [*Kivelson and*

Southwood, 1986]. According to *Zhu and Kivelson* [1989] and *Inhester* [1987], the turning point of the wave will be

$$x_t - x_\omega = -\frac{\omega^2 \lambda^2}{[\mathrm{d}V_A^2(x)/\mathrm{d}x]_{x=x_\omega}}, \tag{10}$$

where x_t is the turning point and x_ω is the position of resonance on the field line. The gradient of Alfvén velocity will be largest near the plasmapause. As an estimation, we calculate the variation of V_A from satellite data and choose the average $\Delta V_A/\Delta x$ as the velocity gradient. The turning point should be in the place of $x_t \sim x_\omega + 1.108$Re, implying that wave energy absorption should be considerable in such a situation. The conclusion is that there should be two effects that cause the wave to be damped in the waveguide, the wave energy absorption effect and the wave energy decreasing effect, over greater propagation distance as waves are reflected at waveguide boundaries before reaching the spacecraft. The situation is, in general, more complicated because of the geometry of the waveguide and the fact that the source of waves is unlikely to be point-like. Nevertheless, based on our simple estimates the conclusion is that propagation effects leading to loss of energy cannot explain the energy loss from waves that are observed.

4. Conclusion

In this study, we have examined ULF wave damping mechanisms that include ionospheric joule heating, Landau damping, and waveguide energy propagation. The mechanisms have been evaluated for two interplanetary shock-related ULF wave events observed by Cluster on 7 November 2004 and 30 August 2001. In the two events studied, we discuss mechanisms for damping of ULF waves. Specifically, using expressions in the published literature, we show that among Landau damping, joule heating, and wave propagation, Landau damping can best explain the rates observed. The experimental facts stemming from the interplanetary shock impacts, and the resulting fast-damped ULF waves that are observed, can be summarized as follows:

1. In the event on 7 November 2004, the four Cluster spacecraft observed intense ULF waves with a period of about 100–150 s near the plasmasphere boundary layer after the arrival of the interplanetary shock. The resulting Alfvén waves with strong poloidal components can accelerate particles effectively [*Zong et al.*, 2009] and were damped very fast within several hundred seconds. In the event on 30 October 2001, C1, C2, and C4 observed relatively weak shock-induced ULF waves in the plasmasphere. C3 observed the same event in the plasmasphere boundary layer. By comparing the power of observed waves, it is found that Alfvén waves are damped faster in the plasmasphere boundary layer than within the plasmasphere in this event. The redistribution effect of plasma near the plasmapause is omitted in this study.
2. Joule heating is found to be significant in the two events studied but cannot account for the fast damping of ULF waves that are observed. The damping rate due to joule heating maintained, in general, the same rate in the plasmasphere and plasmasphere boundary layer.
3. Drift-bounce resonant (Landau damping) interactions between Alfvén waves and different kinds of particles provide an effective ULF wave energy exchange process. For the events considered, ULF wave damping rates for O+ in the range of a few to several keV are large enough to explain damping rates of waves observed by Cluster. The energy of O+ ions satisfying the drift-bounce resonance condition coincides with a resonance peak in ion flux modulations in the 7 November 2004 and 30 August 2001 events observed by Cluster. In the event on 30 August 2001, Landau damping is also higher in the plasmasphere boundary layer than in the plasmasphere. The observed higher damping rates in the plasmasphere boundary layer can be explained by the higher proportion of Landau resonant ions present in that region. It can be concluded that fast Landau damping of shock-induced ULF waves occurs preferentially in the plasmasphere boundary layer region.

Acknowledgments
We are grateful to the Cluster Active Archive community (http://caa.estec.esa.int/caa/home.xml) for the Cluster data used in this study. The authors thank Y. F. Wang, I. Vogiatzis, and A. T. Y. Lui for helpful discussions during the preparation of this paper. This work was supported by the National Natural Science Foundation of China (41421003) and Major Project of Chinese National Programs for Fundamental Research and Development (2012CB825603). R. Rankin is supported in this research through funding from the Canadian Space Agency and the Natural Sciences and Engineering Research Council of Canada.

Larry Kepko thanks the reviewers for their assistance in evaluating this paper.

References

Allan, W., and F. B. Knox (1979), A dipole field model for axisymmetric Alfven waves with finite ionosphere conductivities, *Planet. Space Sci.*, *27*, 79–85, doi:10.1016/0032-0633(79)90149-1.

Balogh, A., et al. (2001), The cluster magnetic field investigation: Overview of in-flight performance and initial results, *Ann. Geophys.*, *19*, 1207–1217, doi:10.5194/angeo-19-1207-2001.

Baumjohann, W., and R. A. Treumann (1997), *Basic Space Plasma Physics*, Imperial College Press, London, U. K.

Brito, T., L. Woodger, M. Hudson, and R. Millan (2012), Energetic radiation belt electron precipitation showing ULF modulation, *Geophys. Res. Lett.*, *39*, L22104, doi:10.1029/2012GL053790.

Chen, L., and A. Hasegawa (1988), On magnetospheric hydromagnetic waves excited by energetic ring-current particles, *J. Geophys. Res.*, *93*(A8), 8763–8767, doi:10.1029/JA093iA08p08763.

Claudepierre, S. G., S. R. Elkington, and M. Wiltberger (2008), Solar wind driving of magnetospheric ULF waves: Pulsations driven by velocity shear at the magnetopause, *J. Geophys. Res.*, *113*, A05218, doi:10.1029/2007JA012890.

Claudepierre, S. G., M. Wiltberger, S. R. Elkington, W. Lotko, and M. K. Hudson (2009), Magnetospheric cavity modes driven by solar wind dynamic pressure fluctuations, *Geophys. Res. Lett.*, *36*, L13101, doi:10.1029/2009GL039045.

Claudepierre, S. G., M. K. Hudson, W. Lotko, J. G. Lyon, and R. E. Denton (2010), Solar wind driving of magnetospheric ULF waves: Field line resonances driven by dynamic pressure fluctuations, *J. Geophys. Res.*, *115*, A11202, doi:10.1029/2010JA015399.

Claudepierre, S. G., et al. (2013), Van Allen Probes observation of localized drift resonance between poloidal mode ultra-low frequency waves and 60 keV electrons, *Geophys. Res. Lett.*, *40*, 4491–4497, doi:10.1002/grl.50901.

Dungey, J. W. (1955), *Electrodynamics of the Outer Atmosphere*, 229 pp., Ionosphere Res. Lab., Pennsylvania State Univ.

Elkington, S. R., M. K. Hudson, and A. A. Chan (1999), Acceleration of relativistic electrons via drift-resonant interaction with toroidal-mode Pc-5 ULF oscillations, *Geophys. Res. Lett.*, *26*, 3273–3276, doi:10.1029/1999GL003659.

Elkington, S. R., M. K. Hudson, M. J. Wiltberger, and J. G. Lyon (2002), MHD/particle simulations of radiation belt dynamics, *J. Atmos. Sol. Terr. Phys.*, *64*, 607–615, doi:10.1016/S1364-6826(02)00018-4.

Elkington, S. R., M. K. Hudson, and A. A. Chan (2003), Resonant acceleration and diffusion of outer zone electrons in an asymmetric geomagnetic field, *J. Geophys. Res.*, *108*(A3), 1116, doi:10.1029/2001JA009202.

Elkington, S. R., M. Wiltberger, A. A. Chan, and D. N. Baker (2004), Physical models of the geospace radiation environment, *J. Atmos. Sol. Terr. Phys.*, *66*, 1371–1387, doi:10.1016/j.jastp.2004.03.023.

Eriksson, P. T. I., L. G. Blomberg, S. Schaefer, and K.-H. Glassmeier (2006), On the excitation of ULF waves by solar wind pressure enhancements, *Ann. Geophys.*, *24*, 3161–3172, doi:10.5194/angeo-24-3161-2006.

Evans, R. M., M. Opher, V. Jatenco-Pereira, and T. I. Gombosi (2009), Surface Alfvén wave damping in a three-dimensional simulation of the solar wind, *Astrophys. J.*, *703*, 179–186, doi:10.1088/0004-637X/703/1/179.

Fairfield, D. H., A. Otto, T. Mukai, S. Kokubun, R. P. Lepping, J. T. Steinberg, A. J. Lazarus, and T. Yamamoto (2000), Geotail observations of the Kelvin-Helmholtz instability at the equatorial magnetotail boundary for parallel northward fields, *J. Geophys. Res.*, *105*, 21,159–21,174, doi:10.1029/1999JA000316.

Fraser, B. J., J. L. Horwitz, J. A. Slavin, Z. C. Dent, and I. R. Mann (2005), Heavy ion mass loading of the geomagnetic field near the plasmapause and ULF wave implications, *Geophys. Res. Lett.*, *32*, L04102, doi:10.1029/2004GL021315.

Greenwald, R. A., and A. D. M. Walker (1980), Energetics of long period resonant hydromagnetic waves, *Geophys. Res. Lett.*, *7*, 745–748, doi:10.1029/GL007i010p00745.

Hasegawa, H., M. Fujimoto, T.-D. Phan, H. Rème, A. Balogh, M. W. Dunlop, C. Hashimoto, and R. TanDokoro (2004), Transport of solar wind into Earth's magnetosphere through rolled-up Kelvin-Helmholtz vortices, *Nature*, *430*, 755–758, doi:10.1038/nature02799.

Hollweg, J. V. (1971), Nonlinear Landau damping of Alfvén waves, *Phys. Rev. Lett.*, *27*, 1349–1352, doi:10.1103/PhysRevLett.27.1349.

Hudson, M., R. Denton, M. Lessard, E. Miftakhova, and R. Anderson (2004), A study of Pc-5 ULF oscillations, *Ann. Geophys.*, *22*, 289–302, doi:10.5194/angeo-22-289-2004.

Inhester, B. (1987), Numerical modeling of hydromagnetic wave coupling in the magnetosphere, *J. Geophys. Res.*, *92*, 4751–4756, doi:10.1029/JA092iA05p04751.

James, M. K., T. K. Yeoman, P. N. Mager, and D. Y. Klimushkin (2013), The spatio-temporal characteristics of ULF waves driven by substorm injected particles, *J. Geophys. Res. Space Physics*, *118*, 1737–1749, doi:10.1002/jgra.50131.

Jordanova, V. K., L. M. Kistler, J. U. Kozyra, G. V. Khazanov, and A. F. Nagy (1996), Collisional losses of ring current ions, *J. Geophys. Res.*, *101*, 111–126, doi:10.1029/95JA02000.

Kepko, L., and H. E. Spence (2003), Observations of discrete, global magnetospheric oscillations directly driven by solar wind density variations, *J. Geophys. Res.*, *108*(A6), 1257, doi:10.1029/2002JA009676.

Kivelson, M. G., and D. J. Southwood (1986), Coupling of global magnetospheric MHD eigenmodes to field line resonances, *J. Geophys. Res.*, *91*, 4345–4351, doi:10.1029/JA091iA04p04345.

Li, X., I. Roth, M. Temerin, J. R. Wygant, M. K. Hudson, and J. B. Blake (1993), Simulation of the prompt energization and transport of radiation belt particles during the March 24, 1991 SSC, *Geophys. Res. Lett.*, *20*, 2423–2426, doi:10.1029/93GL02701.

Loto'aniu, T. M., I. R. Mann, L. G. Ozeke, A. A. Chan, Z. C. Dent, and D. K. Milling (2006), Radial diffusion of relativistic electrons into the radiation belt slot region during the 2003 Halloween geomagnetic storms, *J. Geophys. Res.*, *111*, A04218, doi:10.1029/2005JA011355.

Lysak, R. L., and W. Lotko (1996), On the kinetic dispersion relation for shear Alfvén waves, *J. Geophys. Res.*, *101*, 5085–5094, doi:10.1029/95JA03712.

Menk, F. W., I. R. Mann, A. J. Smith, C. L. Waters, M. A. Clilverd, and D. K. Milling (2004), Monitoring the plasmapause using geomagnetic field line resonances, *J. Geophys. Res.*, *109*, A04216, doi:10.1029/2003JA010097.

Moullard, O., A. Masson, H. Laakso, M. Parrot, P. Décréau, O. Santolik, and M. Andre (2002), Density modulated whistler mode emissions observed near the plasmapause, *Geophys. Res. Lett.*, *29*(20), 1975, doi:10.1029/2002GL015101.

Newton, R. S., D. J. Southwood, and W. J. Hughes (1978), Damping of geomagnetic pulsations by the ionosphere, *Planet. Space Sci.*, *26*, 201–209, doi:10.1016/0032-0633(78)90085-5.

Odera, T. (1986), Solar wind controlled pulsations: A review, *Rev. Geophys.*, *24*, 55–74.

Rae, I. J., et al. (2005), Evolution and characteristics of global Pc5 ULF waves during a high solar wind speed interval, *J. Geophys. Res.*, *110*, A12211, doi:10.1029/2005JA011007.

Rae, I. J., C. E. J. Watt, F. R. Fenrich, I. R. Mann, L. G. Ozeke, and A. Kale (2007), Energy deposition in the ionosphere through a global field line resonance, *Ann. Geophys.*, *25*, 2529–2539.

Rankin, R., C. E. J. Watt, and J. C. Samson (2007), Self-consistent wave-particle interactions in dispersive scale long-period field-line-resonances, *Geophys. Res. Lett.*, *34*, L23103, doi:10.1029/2007GL031317.

Sciffer, M. D., C. L. Waters, and F. W. Menk (2005), A numerical model to investigate the polarisation azimuth of ULF waves through an ionosphere with oblique magnetic fields, *Ann. Geophys.*, *23*, 3457–3471, doi:10.5194/angeo-23-3457-2005.

Southwood, D., J. Dungey, and R. Etherington (1969), Bounce resonant interaction between pulsations and trapped particles, *Planet. Space Sci.*, *17*(3), 349–361, doi:10.1016/0032-0633(69)90068-3.

Southwood, D. J. (1976), A general approach to low-frequency instability in the ring current plasma, *J. Geophys. Res.*, *81*, 3340–3348, doi:10.1029/JA081i019p03340.

Southwood, D. J., and W. J. Hughes (1983), Theory of hydromagnetic waves in the magnetosphere, *Space Sci. Rev.*, *35*, 301–366, doi:10.1007/BF00169231.

Southwood, D. J., and M. G. Kivelson (1981), Charged particle behavior in low-frequency geomagnetic pulsations. I. Transverse waves, *J. Geophys. Res.*, *86*, 5643–5655, doi:10.1029/JA086iA07p05643.

Southwood, D. J., and M. G. Kivelson (1982), Charged particle behavior in low-frequency geomagnetic pulsations. II. Graphical approach, *J. Geophys. Res.*, *87*, 1707–1710, doi:10.1029/JA087iA03p01707.

Southwood, D. J., J. W. Dungey, and R. J. Etherington (1969), Bounce resonant interaction between pulsations and trapped particles, *Planet. Space Sci.*, *17*, 349–361, doi:10.1016/0032-0633(69)90068-3.

Stix, T. H. (1992), *Waves in Plasmas*, Am. Inst. of Phys., Melville, New York.

Sydorenko, D., and R. Rankin (2012), Simulation of ionospheric disturbances created by Alfvén waves, *J. Geophys. Res.*, *117*, A09229, doi:10.1029/2012JA017693.

Takahashi, K., and A. Y. Ukhorskiy (2007), Solar wind control of Pc5 pulsation power at geosynchronous orbit, *J. Geophys. Res.*, *112*, A11205, doi:10.1029/2007JA012483.

Takahashi, K., P. R. Higbie, and D. N. Baker (1985), Azimuthal propagation and frequency characteristic of compressional Pc 5 waves observed at geostationary orbit, *J. Geophys. Res.*, *90*, 1473–1485, doi:10.1029/JA090iA02p01473.

Takahashi, K., R. W. McEntire, A. T. Y. Lui, and T. A. Potemra (1990), Ion flux oscillations associated with a radially polarized transverse Pc 5 magnetic pulsation, *J. Geophys. Res.*, *95*, 3717–3731, doi:10.1029/JA095iA04p03717.

Tan, L. C., S. F. Fung, and X. Shao (2004), Observation of magnetospheric relativistic electrons accelerated by Pc-5 ULF waves, *Geophys. Res. Lett.*, *31*, L14802, doi:10.1029/2004GL019459.

Tan, L. C., X. Shao, A. S. Sharma, and S. F. Fung (2011), Relativistic electron acceleration by compressional-mode ULF waves: Evidence from correlated Cluster, Los Alamos National Laboratory spacecraft, and ground-based magnetometer measurements, *J. Geophys. Res.*, *116*, A07226, doi:10.1029/2010JA016226.

Tsurutani, B. T., E. Echer, F. L. Guarnieri, and J. U. Kozyra (2008), CAWSES November 7–8, 2004, superstorm: Complex solar and interplanetary features in the post-solar maximum phase, *Geophys. Res. Lett.*, *35*, L06S05, doi:10.1029/2007GL031473.

Wang, C., Q. Zong, F. Xiao, Z. Su, Y. Wang, and C. Yue (2011), The relations between magnetospheric chorus and hiss inside and outside the plasmasphere boundary layer: Cluster observation, *J. Geophys. Res.*, *116*, A07221, doi:10.1029/2010JA016240.

Waters, C. L., and M. D. Sciffer (2008), Field line resonant frequencies and ionospheric conductance: Results from a 2-D MHD model, *J. Geophys. Res.*, *113*, A05219, doi:10.1029/2007JA012822.

Wright, A. N. (1994), Dispersion and wave coupling in inhomogeneous MHD waveguides, *J. Geophys. Res.*, *99*, 159–167, doi:10.1029/93JA02206.

Wright, A. N., W. Allan, and P. A. Damiano (2003), Alfvén wave dissipation via electron energization, *Geophys. Res. Lett.*, *30*(16), 1847, doi:10.1029/2003GL017605.

Wygant, J., F. Mozer, M. Temerin, J. Blake, N. Maynard, H. Singer, and M. Smiddy (1994), Large amplitude electric and magnetic field signatures in the inner magnetosphere during injection of 15 MeV electron drift echoes, *Geophys. Res. Lett.*, *21*, 1739–1742, doi:10.1029/94GL00375.

Yang, B., Q.-G. Zong, Y. F. Wang, S. Y. Fu, P. Song, H. S. Fu, A. Korth, T. Tian, and H. Reme (2010), Cluster observations of simultaneous resonant interactions of ULF waves with energetic electrons and thermal ion species in the inner magnetosphere, *J. Geophys. Res.*, *115*, A02214, doi:10.1029/2009JA014542.

Yang, B., Q.-G. Zong, S. Y. Fu, X. Li, A. Korth, H. S. Fu, C. Yue, and H. Reme (2011a), The role of ULF waves interacting with oxygen ions at the outer ring current during storm times, *J. Geophys. Res.*, *116*, A01203, doi:10.1029/2010JA015683.

Yang, B., et al. (2011b), Pitch angle evolutions of oxygen ions driven by storm time ULF poloidal standing waves, *J. Geophys. Res.*, *116*, A03207, doi:10.1029/2010JA016047.

Zhang, X. Y., et al. (2010), ULF waves excited by negative/positive solar wind dynamic pressure impulses at geosynchronous orbit, *J. Geophys. Res.*, *115*, A10221, doi:10.1029/2009JA015016.

Zhu, X., and M. G. Kivelson (1989), Global mode ULF pulsations in a magnetosphere with a nonmonotonic Alfven velocity profile, *J. Geophys. Res.*, *94*, 1479–1485, doi:10.1029/JA094iA02p01479.

Zong, Q., Y. Wang, C. Yuan, B. Yang, C. Wang, and X. Zhang (2011), Fast acceleration of killer electrons and energetic ions by interplanetary shock stimulated ulf waves in the inner magnetosphere, *Chin. Sci. Bull.*, *56*, 1188–1201, doi:10.1007/s11434-010-4308-8.

Zong, Q., Y. Wang, H. Zhang, S. Fu, C. Wang, C. Yuan, and I. Vogiatzis (2012), Fast acceleration of inner magnetospheric hydrogen and oxygen ions by shock induced ulf waves, *J. Geophys. Res.*, *117*, A11206, doi:10.1029/2012JA018024.

Zong, Q.-G., et al. (2007), Ultralow frequency modulation of energetic particles in the dayside magnetosphere, *Geophys. Res. Lett.*, *34*, L12105, doi:10.1029/2007GL029915.

Zong, Q.-G., et al. (2009), Energetic electron response to ULF waves induced by interplanetary shocks in the outer radiation belt, *J. Geophys. Res.*, *114*, A10204, doi:10.1029/2009JA014393.

